Recent Standard Model Results with Photon Final State in CMS

Rong-Shyang Lu
National Taiwan University

30th Anniversary of the Rencontres du Vietnam
Windows on the Universe
August 7-11, 2023

Selected ~~Recent~~ Standard Model Results with Photon Final State in CMS

Rong-Shyang Lu
National Taiwan University

30th Anniversary of the Rencontres du Vietnam
Windows on the Universe
August 7-11, 2023

Outline

- LHC and CMS
- Photon Reconstruction and Identification
- QCD $\gamma + \text{jet}$ Production at CMS
- Electroweak (VBS) $W\gamma$ and $Z\gamma$ production
- Summary

LHC and CMS

LHC - THE BIG TURN ON

The Large Hadron Collider will accelerate two beams of protons (and later lead ions) in opposite directions and collide them head-on at four locations where huge detectors will analyse the debris

https://www.youtube.com/watch?v=pQhbhpU9Wrg
https://youtu.be/BEnaEMMAO_s

CMS

Before the protons or ions enter the main LHC ring, they travel through a series of machines that accelerate them to increasingly higher energies

THE FIRST STEP
starts above ground and involves stripping electrons from atoms of hydrogen gas to make protons. These are sped up to 31.4% of the speed of light in a linear accelerator and then enter the accelerator chain

Linac 50MeV

BOOSTER RING
Accelerates the protons to 91.6% of the speed of light and feeds them into the 200-metre-diameter Proton Synchrotron machine

1.2GeV

PROTON SYNCHROTRON
Almost 50 years old, this machine accelerates protons to 99.93% of the speed of light (25 GeV in energy). For several weeks, starting in late 2009, it will also accelerate lead ions for the ALICE experiment

SUPER PROTON SYNCHROTRON
Located 40 metres underground, the SPS accelerates protons to 99.9998% of the speed of light (450 GeV in energy). It feeds protons both clockwise and anticlockwise into the LHC

LARGE HADRON COLLIDER (LHC)
Designed to accelerate protons to 99.9999991% of the speed of light (7 TeV in energy). The beams will be made to collide in four experimental areas

CERN laboratory

CMS
COMPACT MUON SOLENOID
Number of scientists: More than 2000
Countries involved: 38
Weight: 12,500 tonnes
Size: 21m long, 15m high, 15m wide

Circumference 27km

Circumference 7km

~100 m

TRANSFER TUNNEL

TRANSFER TUNNEL

ALICE
A LARGE ION COLLIDER EXPERIMENT
Number of scientists: More than 1500
Countries involved: 31
Weight: 10,000 tonnes
Size: 26m long, 16m high, 16m wide

ATLAS
A TOROIDAL LHC APPARATUS
Number of scientists: More than 1900
Countries involved: 35

LHCb
LHC BEAUTY
Number of scientists: More than 650
Countries involved: 14
Weight: 5600 tonnes
Size: 21m long, 10m high, 13m wide

30t

23

LHC Luminosity

- In Run1, CMS recorded 6.1fb^{-1} @7TeV and 23.3 fb^{-1} @8TeV.
- Run 2, CMS recorded 163.6 fb^{-1} @13TeV.
- Run3, CMS has recorded more than 62.6 fb^{-1} @13.6TeV.

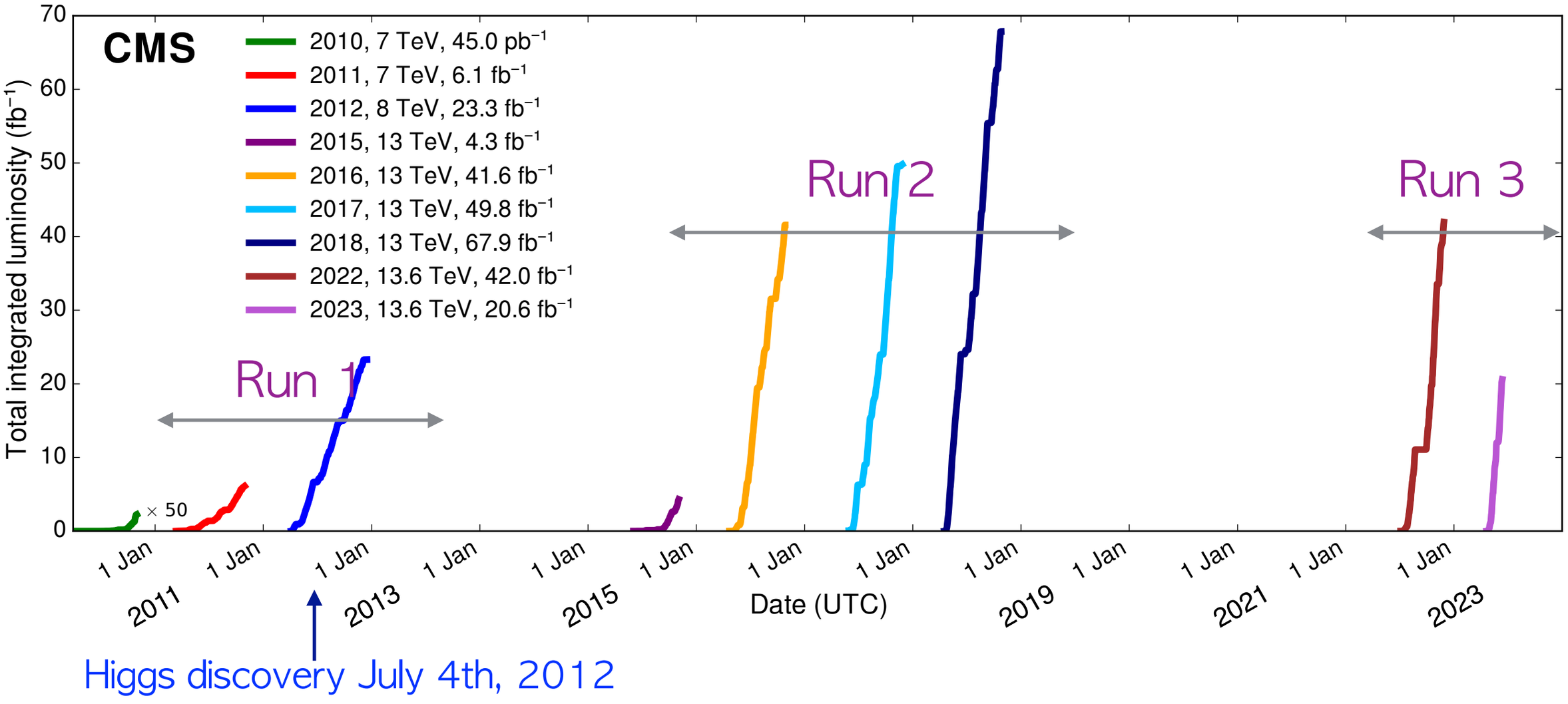

CMS

- General purpose design to detect all particles. Wide reaches of physics potential

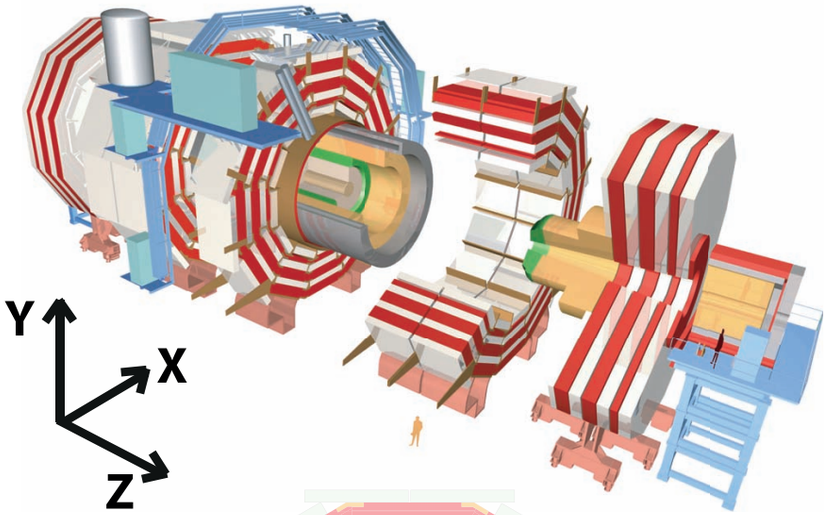

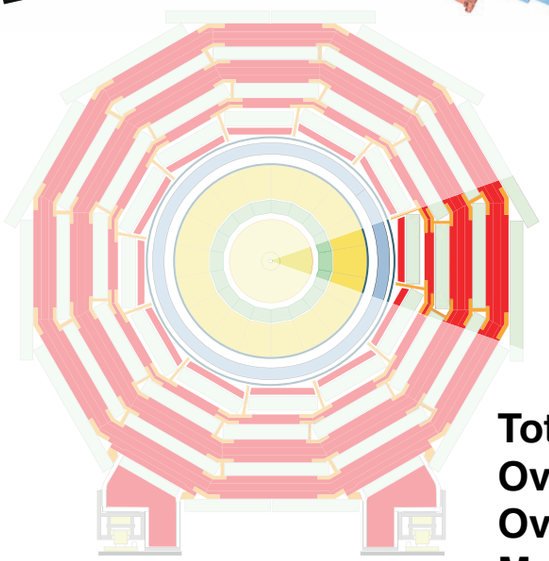

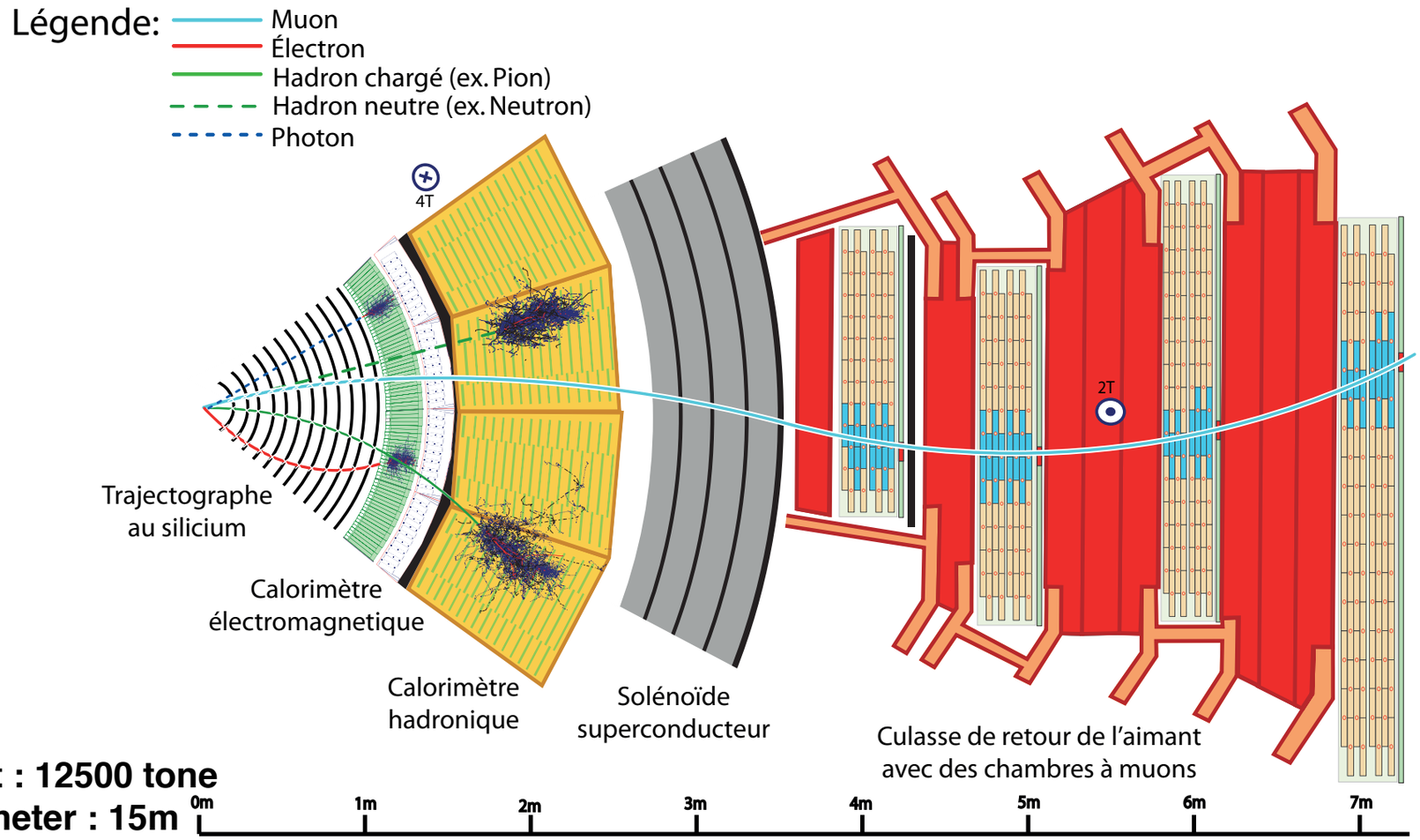

Total weight : 12500 tone
Overall diameter : 15m
Overall length : 21.5m
Magnetic field : 3.8 Tesla

ECAL

- The Electromagnetic Calorimeter of CMS (ECAL)
  - ✦ Homogeneous, compact, hermetic, fine grain $PbWO_4$ crystal calorimeter
  - ✦ Goal is having excellent energy resolution
- Energy resolution of 3x3 crystal matrix

$$\left(\frac{\sigma_E}{E}\right) = \left(\frac{2.8\%\sqrt{GeV}}{\sqrt{E}}\right) \oplus \left(\frac{128\ \mathrm{MeV}}{E}\right) \oplus 0.3\%$$

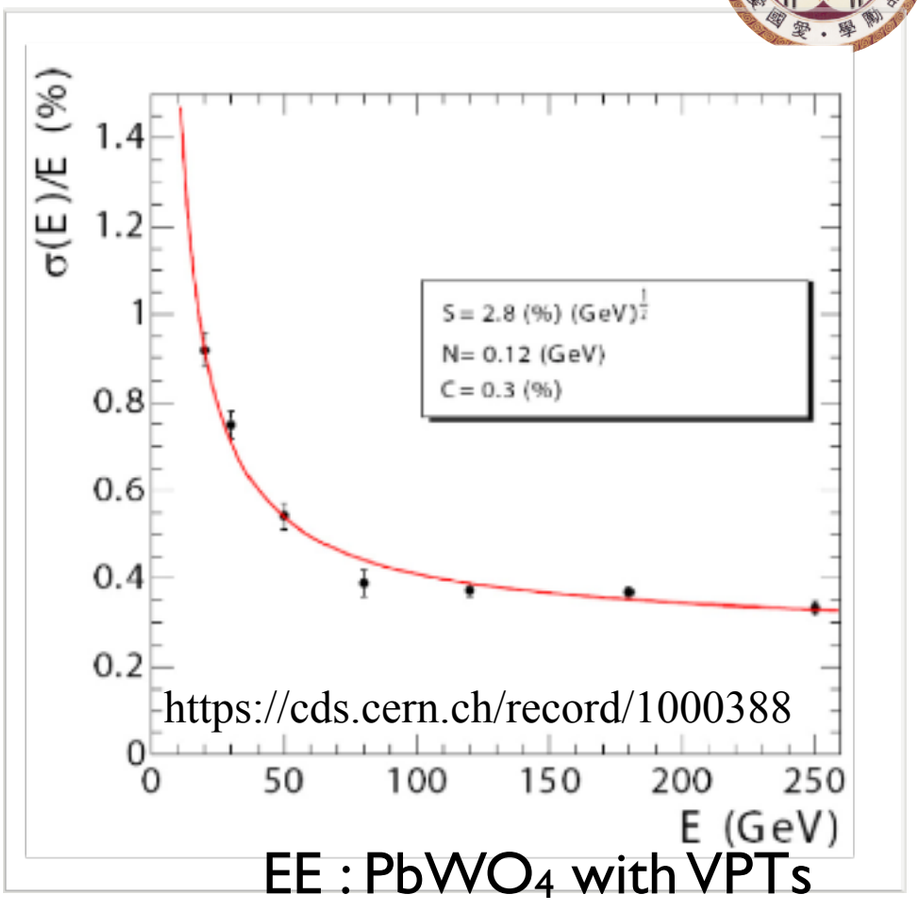

EE : $PbWO_4$ with VPTs
29mm x 29mm x 24.7X_0

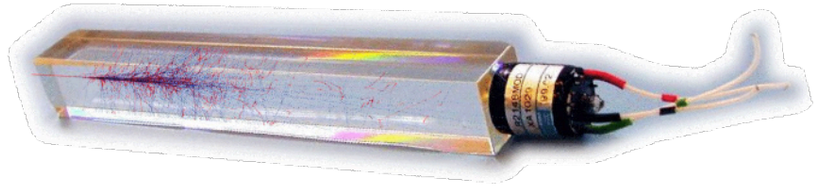

EB : $PbWO_4$ with APDs
22mm x 22mm x 25.8X_0
(Molière radius 22mm)

ES : silicon strip sensors
strip width 1.9mm

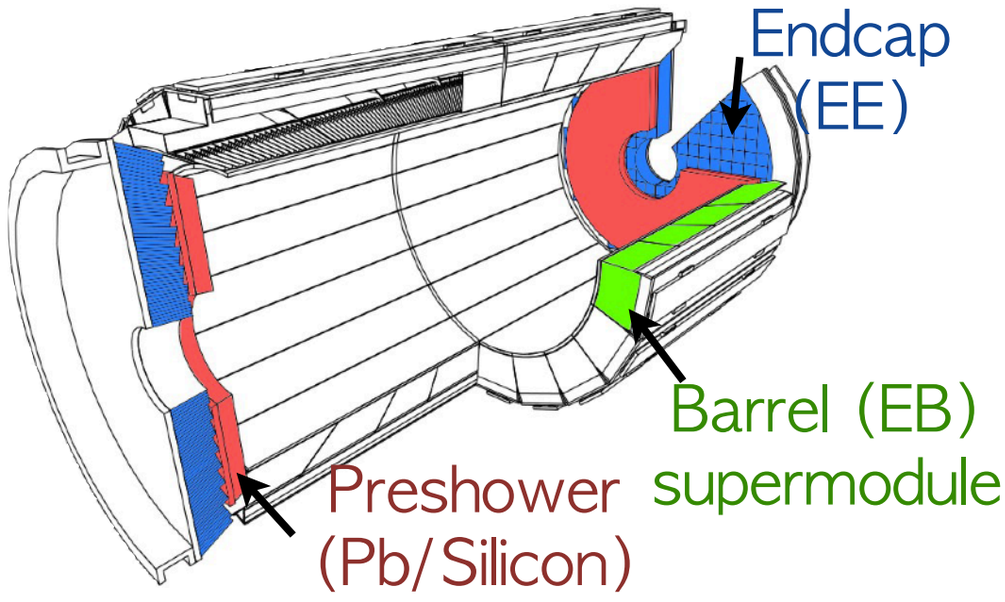

Photon Reconstruction

- Build Basic Cluster with 5x5 crystal matrix. It contains 97% of unconverted photon energy
- 〉50% probability of photon conversion (e+e- pair) in CMS, energy spread into ϕ road due to B filed. Connect basic cluster to form SuperCluster. Barrel : 5 crystal in η and 10-15 crystals in ϕ; Endcap 5x5 crystals + preshower
- Energy deposited by electrons and photons in the ECAL and collected in superclusters is subject to losses
- A correction procedure is needed to calibrate the reconstructed energy back to generated energy.

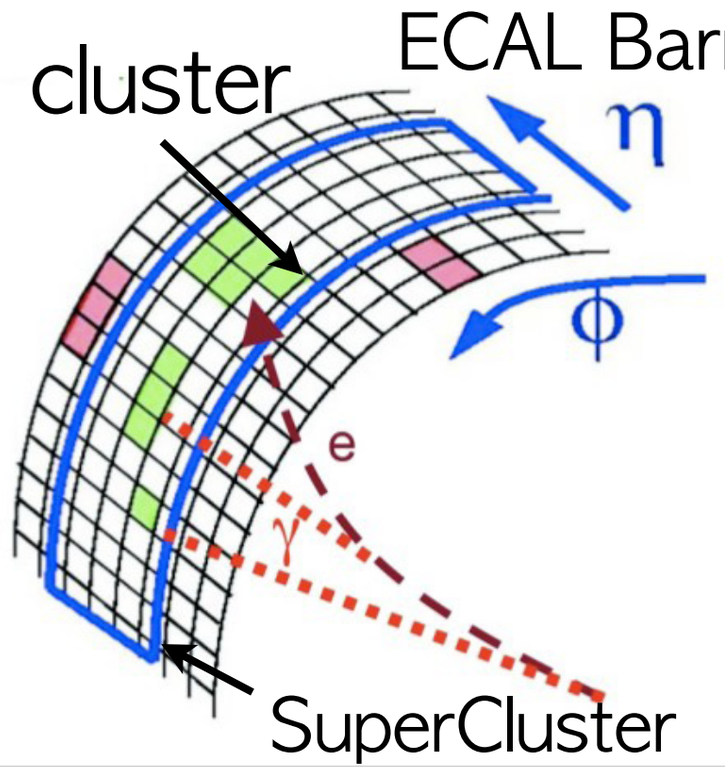

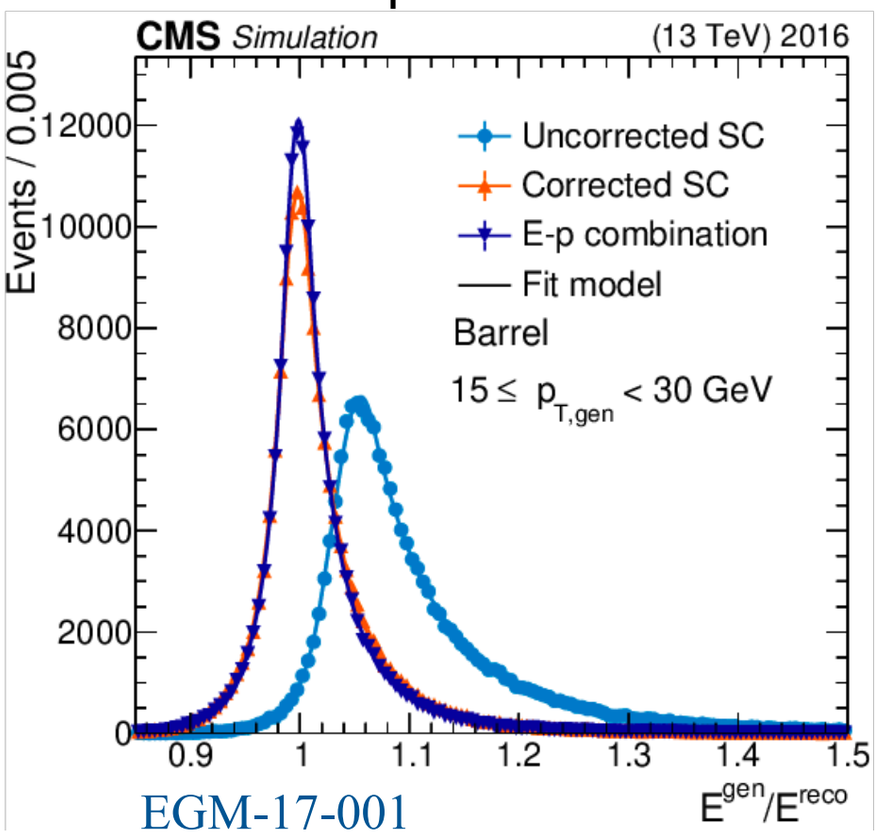

Photon Identification

- Identify a jet fakes a photon
  - ✦ Shower shapes of the cluster, ES shower width in the endcap
  - ✦ Isolation (energy)of photon
  - ✦ Hadronic leakage of photon
- Identify an electron fakes a photon
  - ✦ No pixel hits nor tracks linked with photon
- Cut-based and MVA-BDT-based ID.
- ID trained with MC and compare with data. Overall good agreement between Data and MC

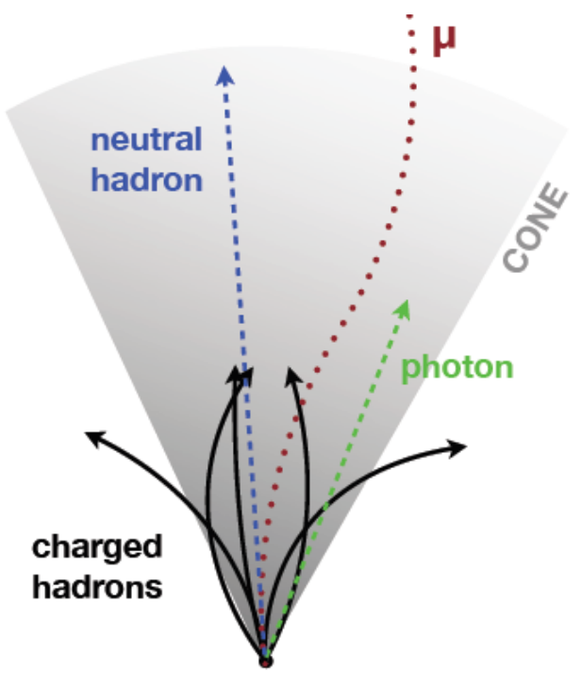

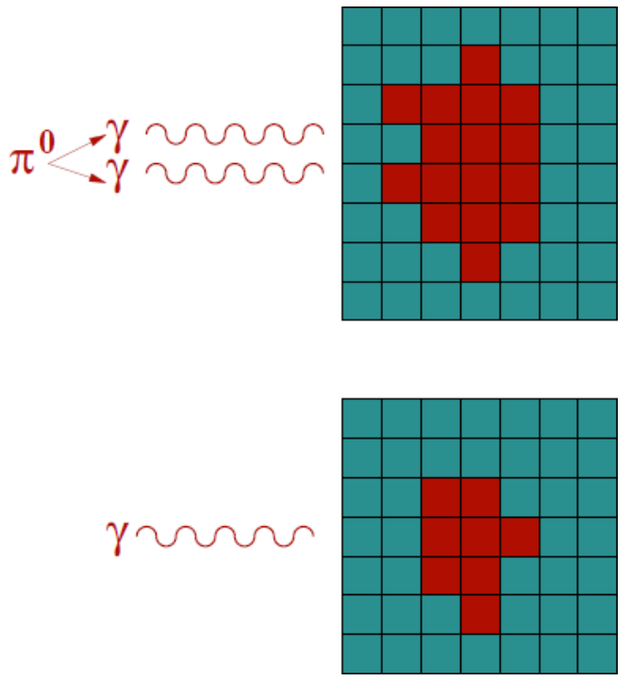

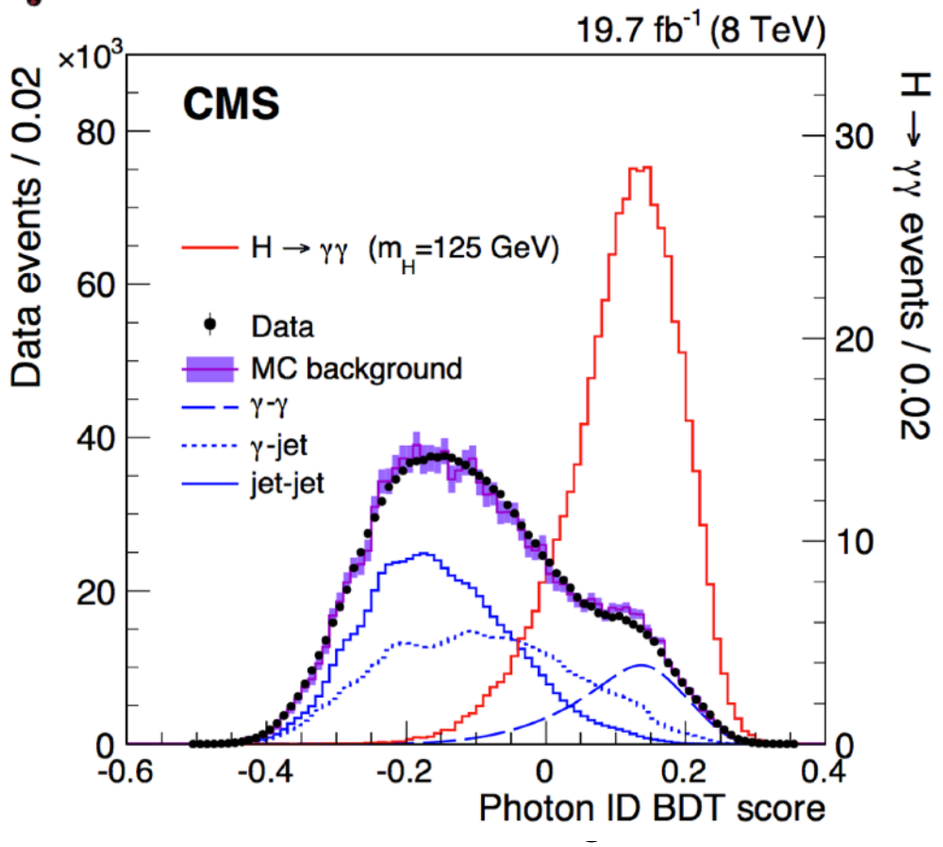

QCD γ + jet Production at CMS

[while LHC acts as a quark-gluon collider]

QCD Photon+jet Production

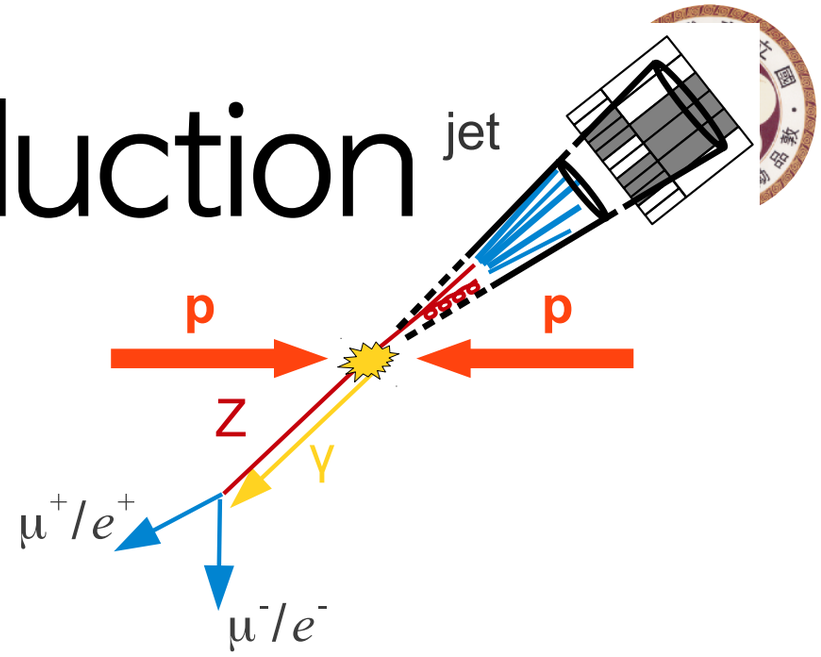

- The photon+jet production is dominated by quark-gluon scattering and sensitive to gluon PDF at medium and high X range

- Compare data cross section with NLO theory prediction, (e.g. JETPHOX with fragmentation at NLO) with different PDFs.

- Also serves as calibration dataset, e.g. jet energy correction.

CMS DP-2020/019

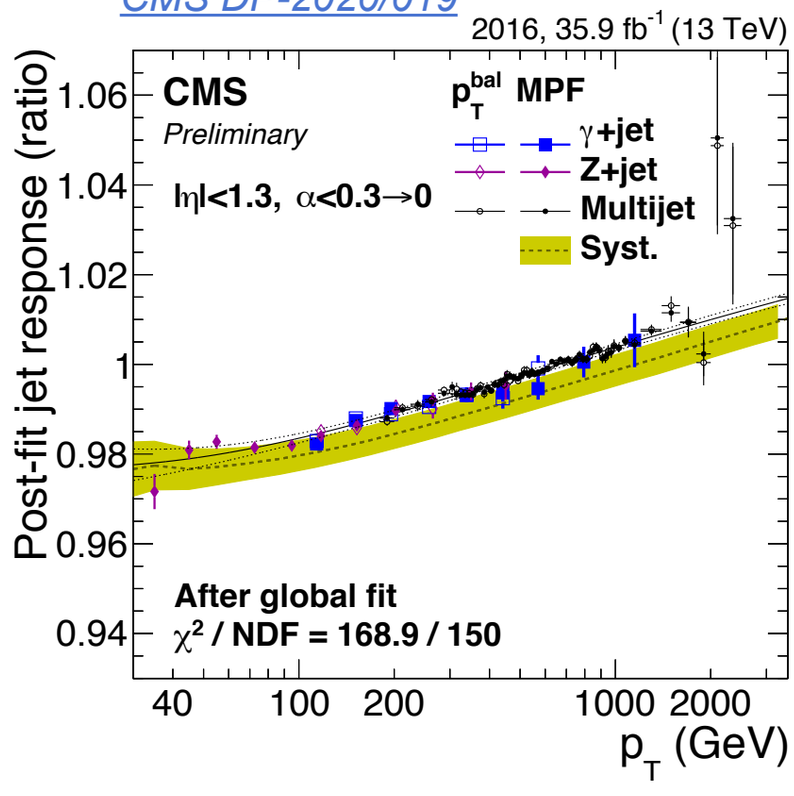

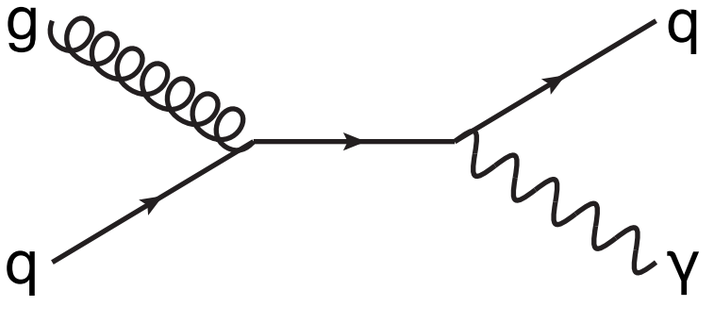

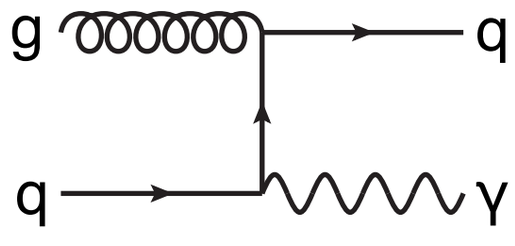

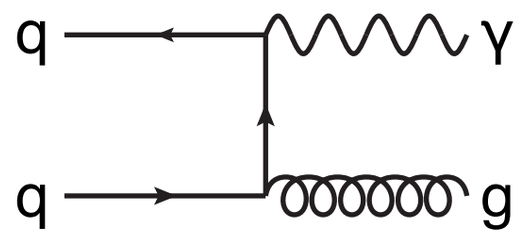

CMS Photon @ 13TeV

- Results of photon and photon+jet production at 13TeV.
- Consistent with JETPHOX (NLO generator) but some feature seen as a function of photon E_T
- NNLO calculation may resolve the dependency.

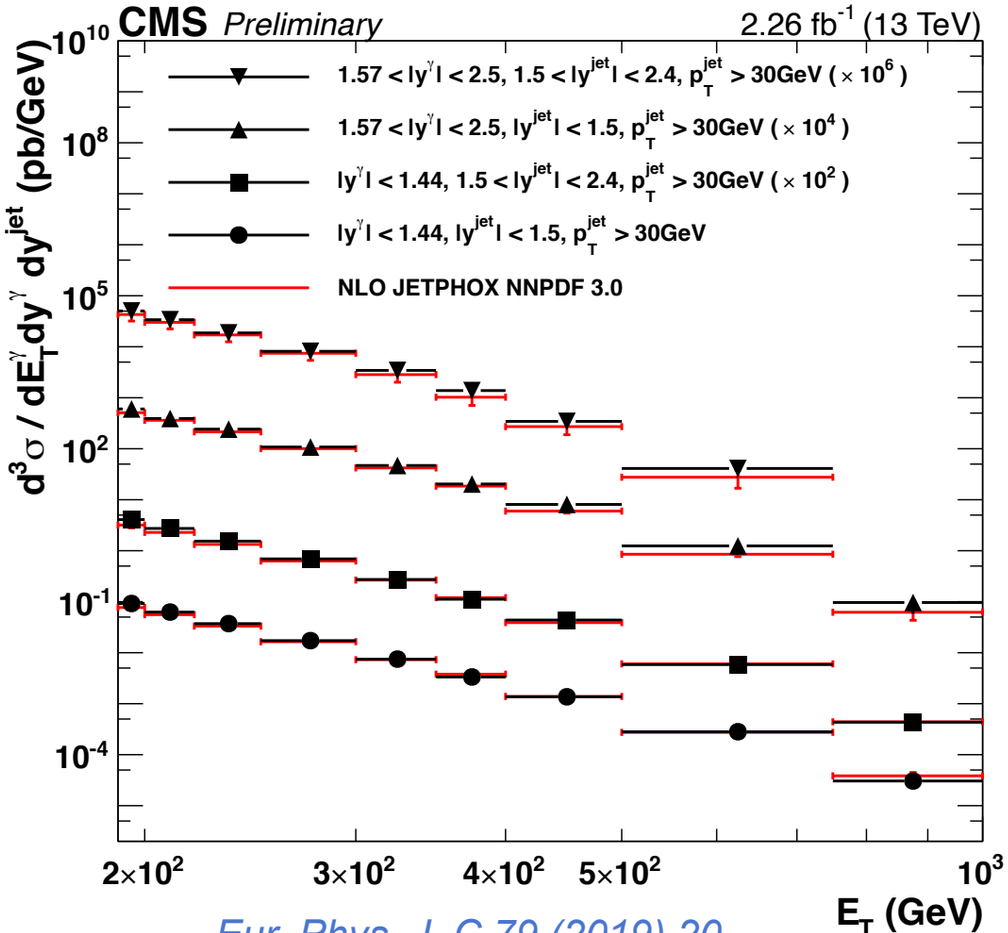

Eur. Phys. J. C 79 (2019) 20

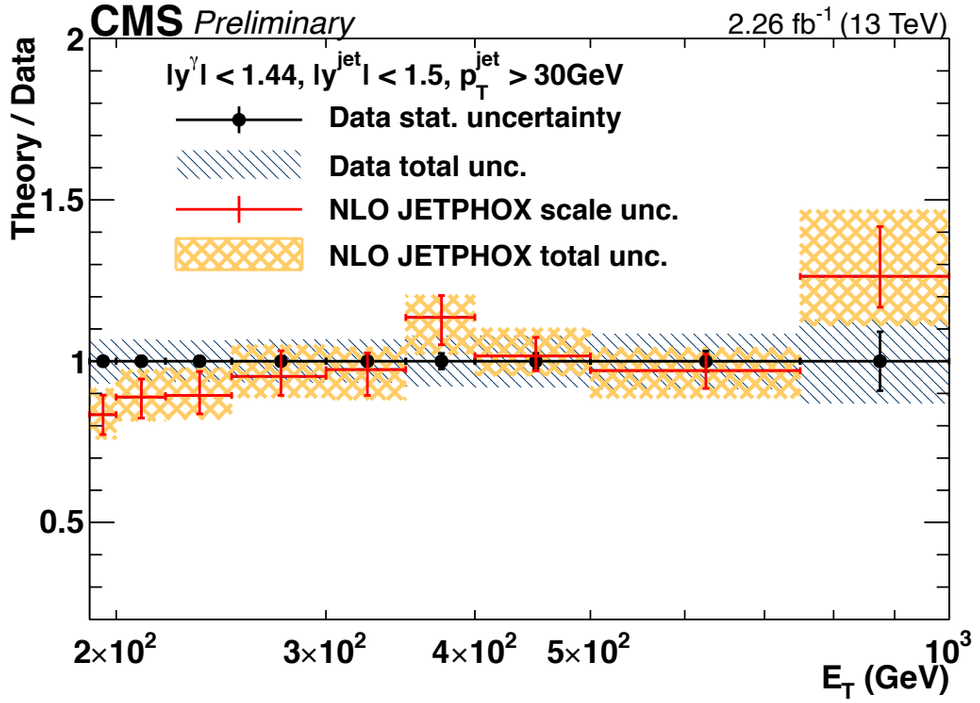

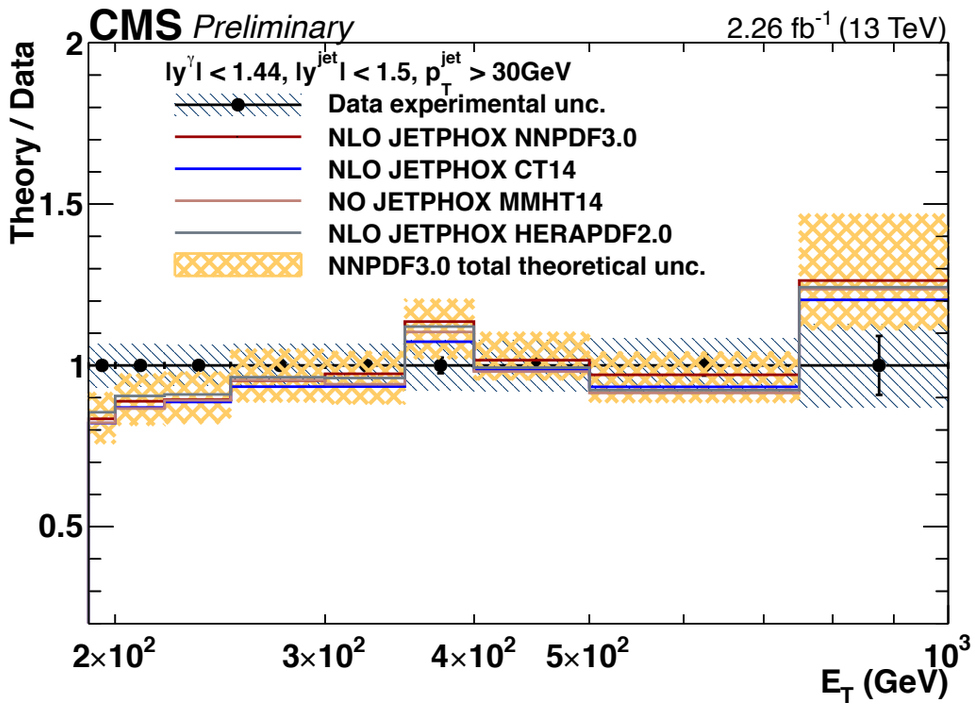

Electroweak (VBS) $W\gamma$ and $Z\gamma$ production

[while LHC acts as a boson-boson collider]

What is VBS signal

- Three contributions at LO for Vector Boson Scattering
  - ✦ Pure EWK：VBS signal
  - ✦ QCD-induced：irreducible background
  - ✦ EWK-QCD interference：add to QCD background

- VBS signature: di-boson production with two very energetic forward-backward QUARK-initiated jets and with large dijet mass (m_{jj}) and rapidity gap

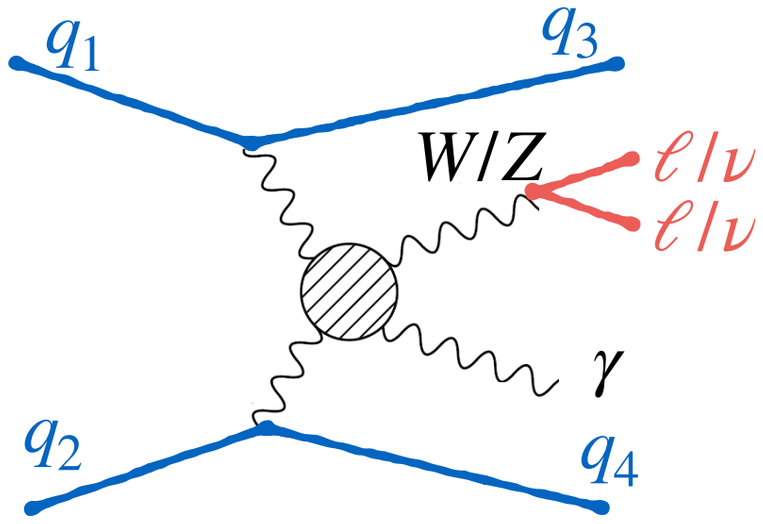

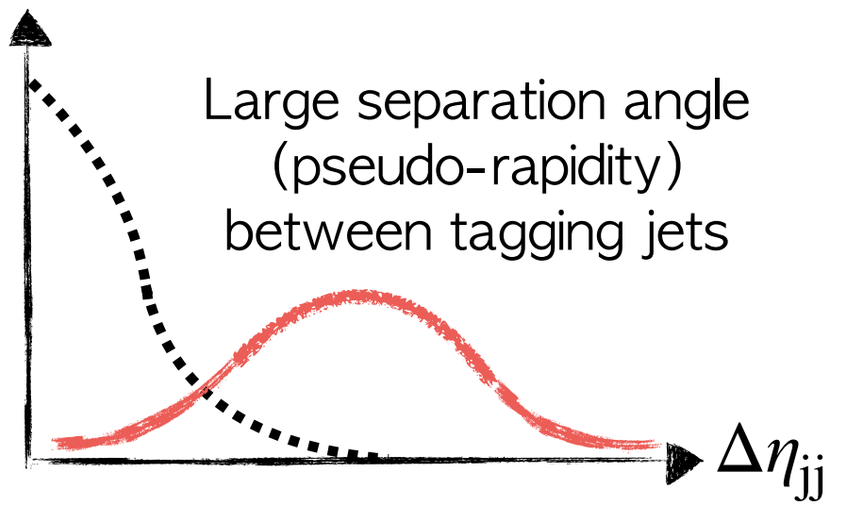

Why is VBS interesting

- Pure Electroweak processes. Provides understanding of the Electroweak sector and complementary to Higgs analyses
  - ✦ Probes gauge interactions：triple and quartic gauge couplings
  - ✦ Probes couplings between Higgs and gauge bosons
- In the EW scale, since no direct evidence of new particle, the recent model-indecent approach with Standard Model effective field theory (SMEFT)
- Parametrize deviations from the SM in terms of Wilson coefficient (c_i) and higher order operators ($\mathcal{O}_i$).

$$\mathcal{L}_{\mathrm{SMEFT}} \sim \mathcal{L}^{(4)}_{\mathrm{SM}} + \frac{1}{\Lambda^2}\sum_i^{(6)} c_i^{(6)}\mathcal{O}_i^{(6)} + \frac{1}{\Lambda^4}\sum_j^{(8)} c_j^{(8)}\mathcal{O}_j^{(8)} + \ldots$$

	WWWW	WWZZ	ZZZZ	WWAZ	WWAA	ZZZA	ZZAA	ZAAA	AAAA
$\mathcal{O}_{S,0}$, $\mathcal{O}_{S,1}$	X	X	X						
$\mathcal{O}_{M,0}$, $\mathcal{O}_{M,1}$,$\mathcal{O}_{M,6}$,$\mathcal{O}_{M,7}$	X	X	X	X	X	X	X		
$\mathcal{O}_{M,2}$,$\mathcal{O}_{M,3}$, $\mathcal{O}_{M,4}$,$\mathcal{O}_{M,5}$		X	X	X	X	X	X		
$\mathcal{O}_{T,0}$,$\mathcal{O}_{T,1}$,$\mathcal{O}_{T,2}$	X	X	X	X	X	X	X	X	X
$\mathcal{O}_{T,5}$,$\mathcal{O}_{T,6}$,$\mathcal{O}_{T,7}$		X	X	X	X	X	X	X	X
$\mathcal{O}_{T,8}$,$\mathcal{O}_{T,9}$			X			X	X	X	X

Table 1-16. *Quartic vertices modified by each dimension-8 operator are marked with X.*

https://doi.org/10.48550/arXiv.1310.6708

CMS VBS results

PROCESS	LUMI [fb^{-1}]	RESULTS	REFERENCE
VBS in ssWW + WZ	Full Run 2 (137/fb)	Observation & XS + dim-8 EFT limits	PLB 809 (2020) 135710
polarized VBS ssWW	Full Run 2 (137/fb)	W_LW_L measurement	PLB 812 (2020) 136018
VBS ZZ	Full Run 2 (137/fb)	Evidence + dim-8	PLB 812 (2021) 135992
VBS osWW	Full Run 2 (137/fb)	Observation & XS	PLB 841 (2023) 137495
VBS VV	Full Run 2 (137/fb)	Evidence	PLB 834 (2022) 137438
VBS VV	2016 data (36/fb)	Dim-8 EFT limits	PLB 798 (2019)134985
VBS Wγ	Full Run 2 (137/fb)	Observation, differential XS + dim-8 EFT limits	PLB 811 (2020) 135988 arXiv : 2212.12592 (accepted by PRD)
VBS Zγ	Full Run 2 (137/fb)	Observation, + dim-8 EFT limits	PRD 104 (2021) 072001
VBS PPS γγWW	Full Run 2 PPS (100/fb)	Dim-6 and dim-8	arXiv:2211.16320, sub. JHEP

This talk

Stringent limits on EFT coefficients

EW $Z(\ell\ell)\gamma$ + jj

PRD 104 (2021) 072001

- VBS signal MC sample generated with MadGraph at LO.
- Signal is selected by the VBS signature.
- Main background from QCD $Z\gamma$jj production. It is modeled using simulation, but constraint with data.
- Background from Z+jets events, with a jet misidentified as a photon, is estimated with data-driven method
- FSR contribution is largely reduced by cutting on $Z\gamma$ invariant mass

Common selection	$p_T^{\ell 1,\ell 2} > 25\,\text{GeV}$, $\lvert\eta^{\ell 1,\ell 2}\rvert < 2.5$ for electron channel $p_T^{\ell 1,\ell 2} > 20\,\text{GeV}$, $\lvert\eta^{\ell 1,\ell 2}\rvert < 2.4$ for muon channel $p_T^{\gamma} > 20\,\text{GeV}$, $\lvert\eta^{\gamma}\rvert < 1.442$ or $1.566 < \lvert\eta^{\gamma}\rvert < 2.500$ $p_T^{j1,j2} > 30\,\text{GeV}$, $\lvert\eta^{j1,j2}\rvert < 4.7$ $70 < m_{\ell\ell} < 110\,\text{GeV}$, $m_{Z\gamma} > 100\,\text{GeV}$ $\Delta R_{jj}, \Delta R_{j\gamma}, \Delta R_{j\ell} > 0.5$, $\Delta R_{\ell\gamma} > 0.7$
Fiducial volume	Common selection, $m_{jj} > 500\,\text{GeV}$, $\lvert\Delta\eta_{jj}\rvert > 2.5$
Control region	Common selection, $150 < m_{jj} < 500\,\text{GeV}$
EW signal region	Common selection, $m_{jj} > 500\,\text{GeV}$, $\lvert\Delta\eta_{jj}\rvert > 2.5$, $\eta^* < 2.4$, $\Delta\phi_{Z\gamma,jj} > 1.9$
aQGC search region	Common selection, $m_{jj} > 500\,\text{GeV}$, $\lvert\Delta\eta_{jj}\rvert > 2.5$, $p_T^{\gamma} > 120\,\text{GeV}$

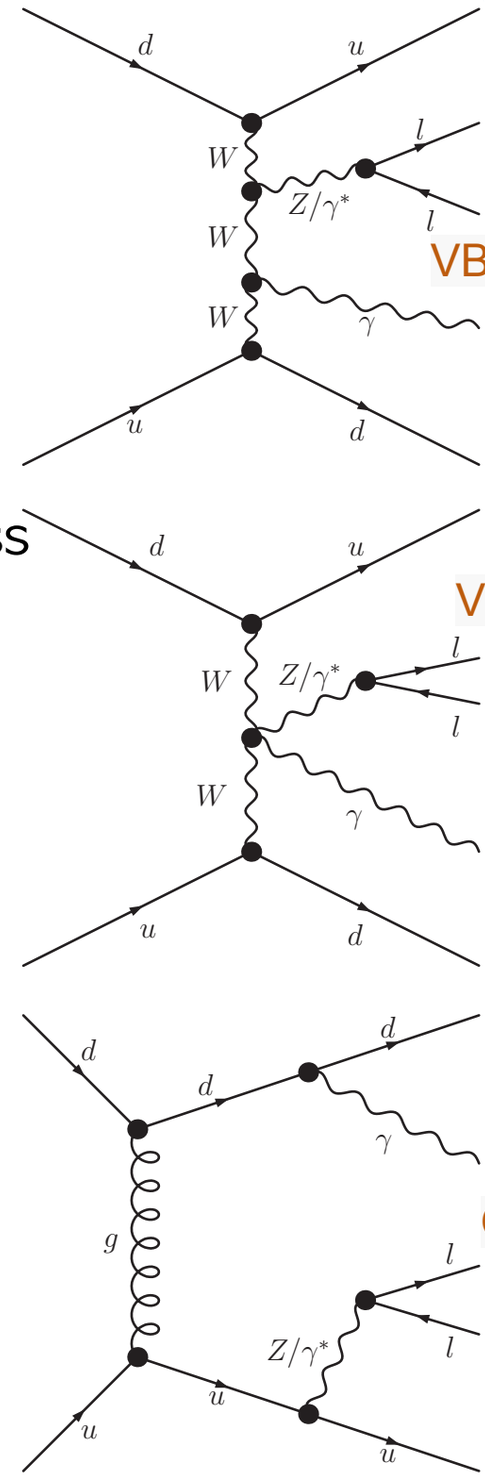

EW $Z(\ell\ell)\gamma + jj$

PRD 104 (2021) 072001

- Observed (expected) significance: 9.4 (8.5)σ
- Inclusive and differential, on p_T^{γ}, $p_T^{\ell_1}$, $p_T^{j_1}$, m_{jj}, cross section are measured. The fiducial cross section measured with signal strength $\hat{\mu}_{EW} = 1.20^{+0.18}_{-0.17}$ is

$$\sigma_{EW}^{EXP} = 5.21 \pm 0.52(stat) \pm 0.56(syst) \text{ fb , where}$$
$$\sigma_{EW}^{TH} = 4.34 \pm 0.26(scale) \pm 0.06(PDF) \text{ fb}$$

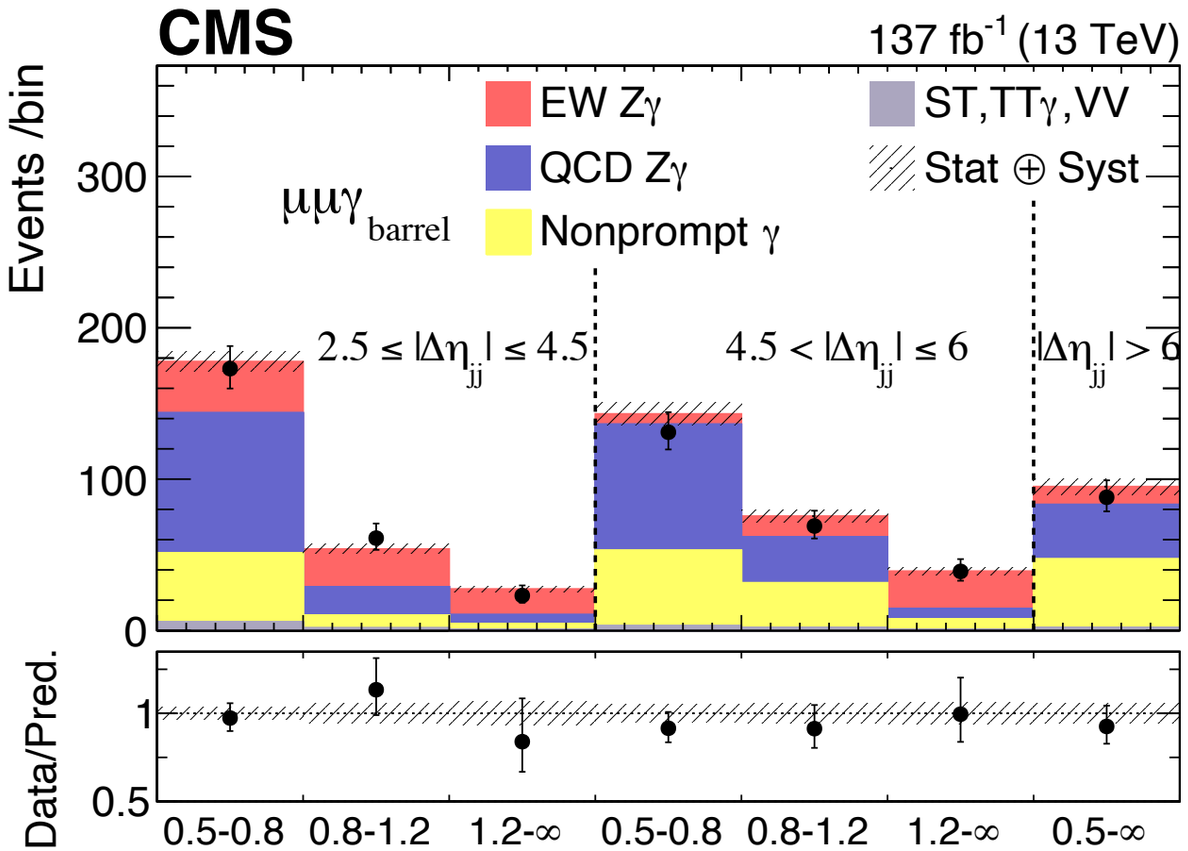

The post-fit 2D distributions of the dimuon for the γ_{barrel} categories.

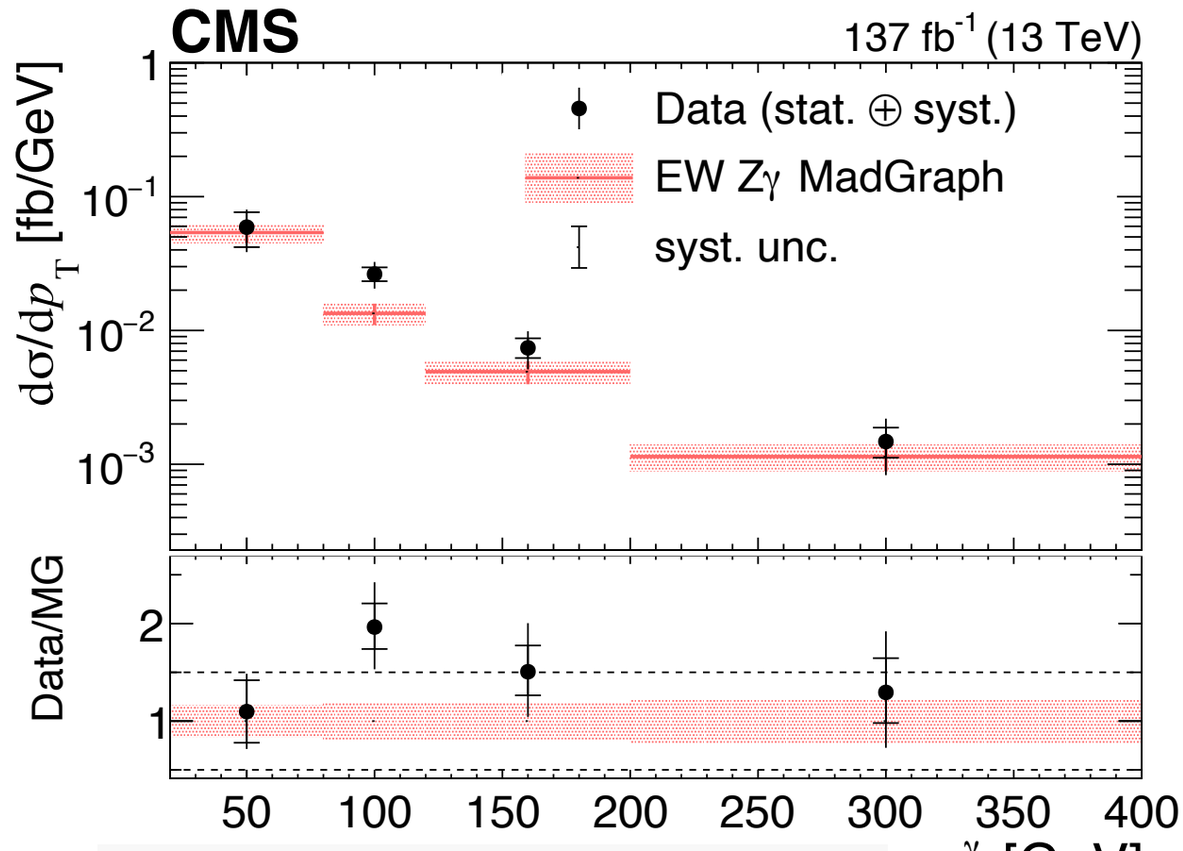

Unfolded differential cross section as a function of leading photon p_T for EW $Z\gamma jj$

EW $Z(\ell\ell)\gamma + jj$

PRD 104 (2021) 072001

- Set limit on aQGC by EFT with events in dedicated search region with high $p_T(>120\,\mathrm{GeV})$ photon.
- Fit on invariant mass of the $Z\gamma$ system

All coupling parameter limits are set in TeV^{-4}, whereas the unitarity bounds are in TeV.

Coupling	Exp. lower	Exp. upper	Obs. lower	Obs. upper	Unitarity bound
F_{M0}/Λ^4	−12.5	12.8	−15.8	16.0	1.3
F_{M1}/Λ^4	−28.1	27.0	−35.0	34.7	1.5
F_{M2}/Λ^4	−5.21	5.12	−6.55	6.49	1.5
F_{M3}/Λ^4	−10.2	10.3	−13.0	13.0	1.8
F_{M4}/Λ^4	−10.2	10.2	−13.0	12.7	1.7
F_{M5}/Λ^4	−17.6	16.8	−22.2	21.3	1.7
F_{M7}/Λ^4	−44.7	45.0	−56.6	55.9	1.6
F_{T0}/Λ^4	−0.52	0.44	−0.64	0.57	1.9
F_{T1}/Λ^4	−0.65	0.63	−0.81	0.90	2.0
F_{T2}/Λ^4	−1.36	1.21	−1.68	1.54	1.9
F_{T5}/Λ^4	−0.45	0.52	−0.58	0.64	2.2
F_{T6}/Λ^4	−1.02	1.07	−1.30	1.33	2.0
F_{T7}/Λ^4	−1.67	1.97	−2.15	2.43	2.2
F_{T8}/Λ^4	−0.36	0.36	−0.47	0.47	1.8
F_{T9}/Λ^4	−0.72	0.72	−0.91	0.91	1.9

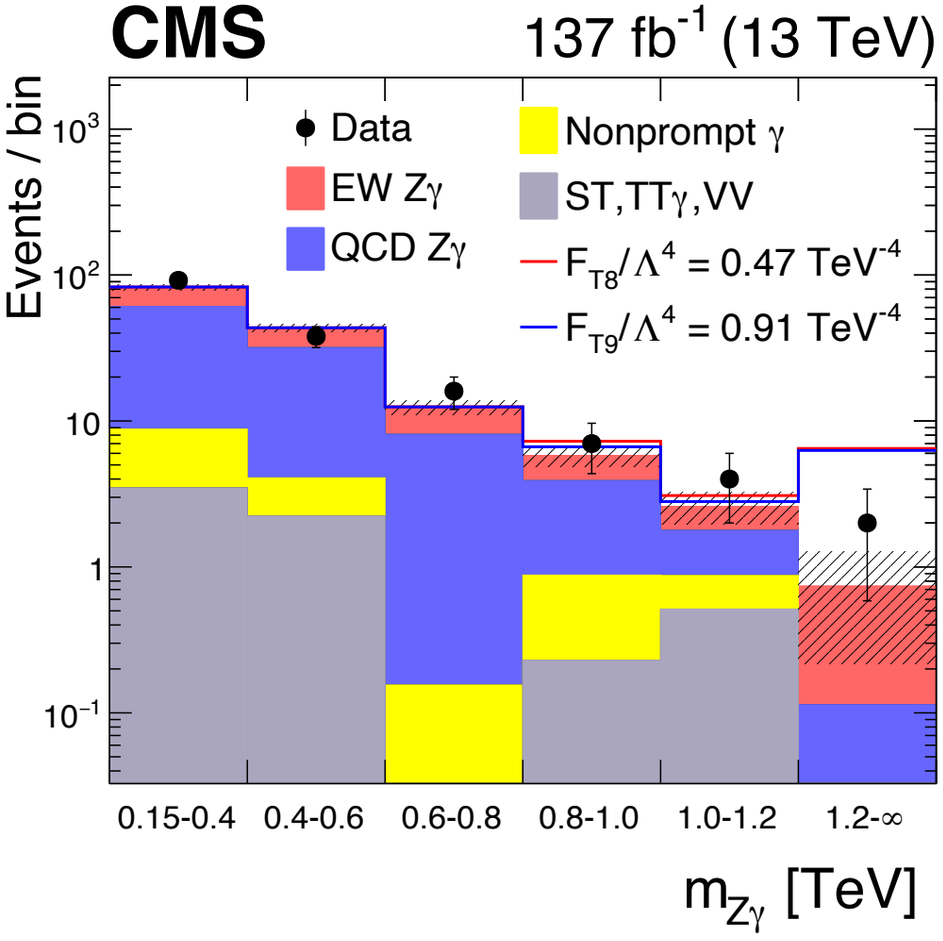

	WWWW	WWZZ	ZZZZ	WWAZ	WWAA	ZZZA	ZZAA	ZAAA	AAAA
$\mathcal{O}_{S,0}$, $\mathcal{O}_{S,1}$	X	X	X						
$\mathcal{O}_{M,0}$, $\mathcal{O}_{M,1}$,$\mathcal{O}_{M,6}$,$\mathcal{O}_{M,7}$	X	X	X	X	X	X	X		
$\mathcal{O}_{M,2}$,$\mathcal{O}_{M,3}$, $\mathcal{O}_{M,4}$,$\mathcal{O}_{M,5}$		X	X	X	X	X	X		
$\mathcal{O}_{T,0}$,$\mathcal{O}_{T,1}$,$\mathcal{O}_{T,2}$	X	X	X	X	X	X	X	X	X
$\mathcal{O}_{T,5}$,$\mathcal{O}_{T,6}$,$\mathcal{O}_{T,7}$		X	X	X	X	X	X	X	X
$\mathcal{O}_{T,8}$,$\mathcal{O}_{T,9}$			X			X	X	X	X

Table 1-16. *Quartic vertices modified by each dimension-8 operator are marked with X.*

EW $W(\ell\nu)\gamma$ + jj

arXiv : 2212.12592
Accepted by PRD

- Measurements using full Run 2 data by CMS, with W leptonic decay
- Signal is generated with MadGraph at LO
- Main backgrounds from QCD $W\gamma$ and non prompt γ/ℓ by data-driven method
- Results extracted from 2D variables of m_{jj} and $m_{\ell j}$. Simultaneous fit in the CR and SR

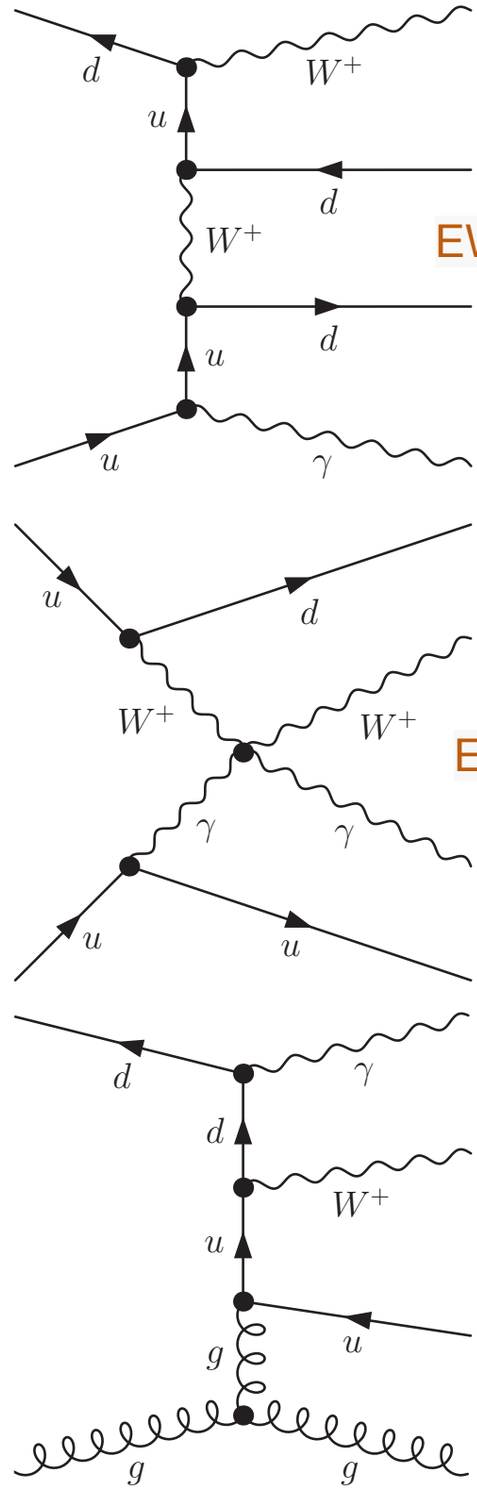

Common selection

- pT(ℓ/γ) > 35 (25) GeV
- Jets with p_T > 50 GeV
- ΔR(ℓ,γ/j/) > 0.5
- m_T(W) > 30 GeV
- MET > 30 GeV
- $|m_{e\gamma} - m_Z|$ > 10 GeV
- $m_{W\gamma}$ > 100 GeV

Control region

- 200 GeV < m_{jj} < 400 GeV

Signal region

- $\Delta\phi(\phi_{Z\gamma},\phi_{jj}) > 2$
- $|\eta_{Z\gamma} - (\eta_{j1} + \eta_{j2})/2| < 1.2$
- m_{jj} > 500 GeV
- $\Delta\eta_{jj}$ > 2.5

EW $W(\ell\nu)\gamma + \mathrm{jj}$

arXiv : 2212.12592
Accepted by PRD

- Observed (expected) significance: 6.0 (6.8)σ
- Inclusive and differential, on p_T^{γ}, $p_T^{\ell_1}$, $p_T^{\mathrm{j}_1}$, $p_T^{\ell\mathrm{j}}$, m_{jj}, $\Delta\eta_{\mathrm{jj}}$, cross section are measured. Fiducial cross section is measured by $\sigma^{\mathrm{fid}} = \sigma_g \hat{\mu} \alpha_{gf}$, where $\sigma_g = 0.776\,\mathrm{pb}$, calculated by MadGraph at LO, acceptance $\alpha_{gf} = 0.034$, and observed signal strength in data $\hat{\mu} = 0.88^{+0.19}_{-0.18}$. This leads to

$$\sigma^{\mathrm{fid}}_{\mathrm{EW}} = 23.5 \pm 2.8(\mathrm{stat})^{+1.9}_{-1.7}(\mathrm{theo})^{+3.5}_{-3.4}(\mathrm{syst})\ \mathrm{fb}$$

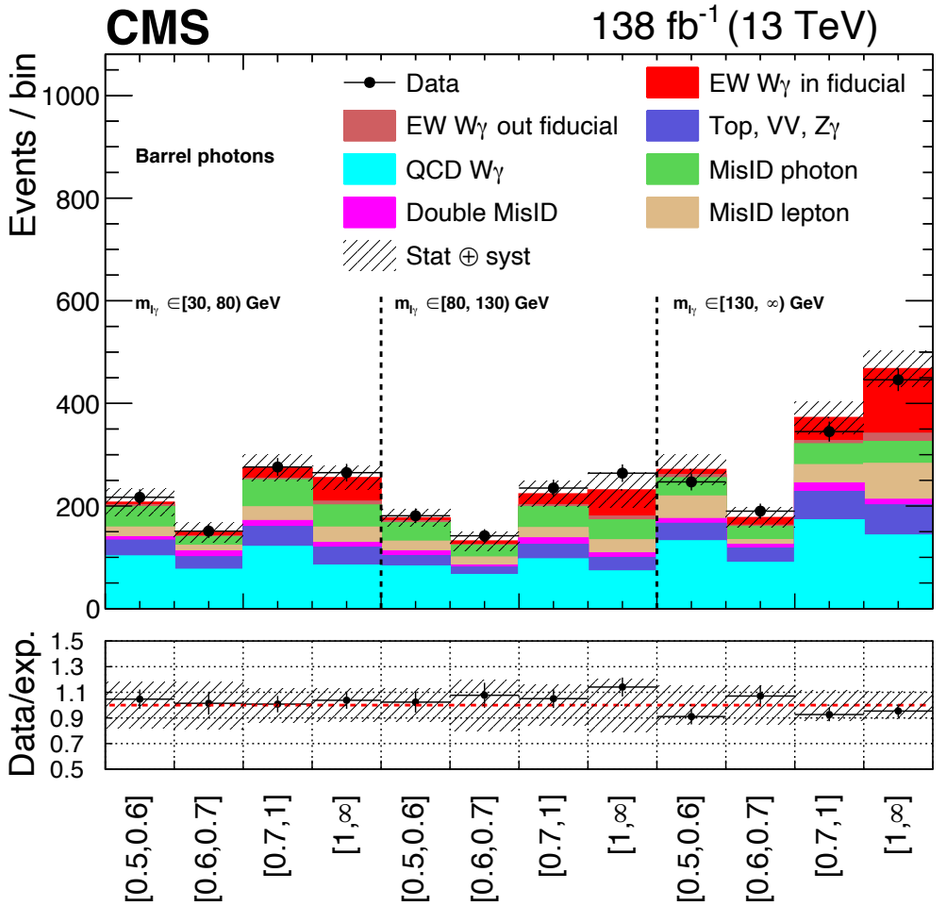

The 2D distribution used in the fit for the total EW $W\gamma$ cross section measurement.

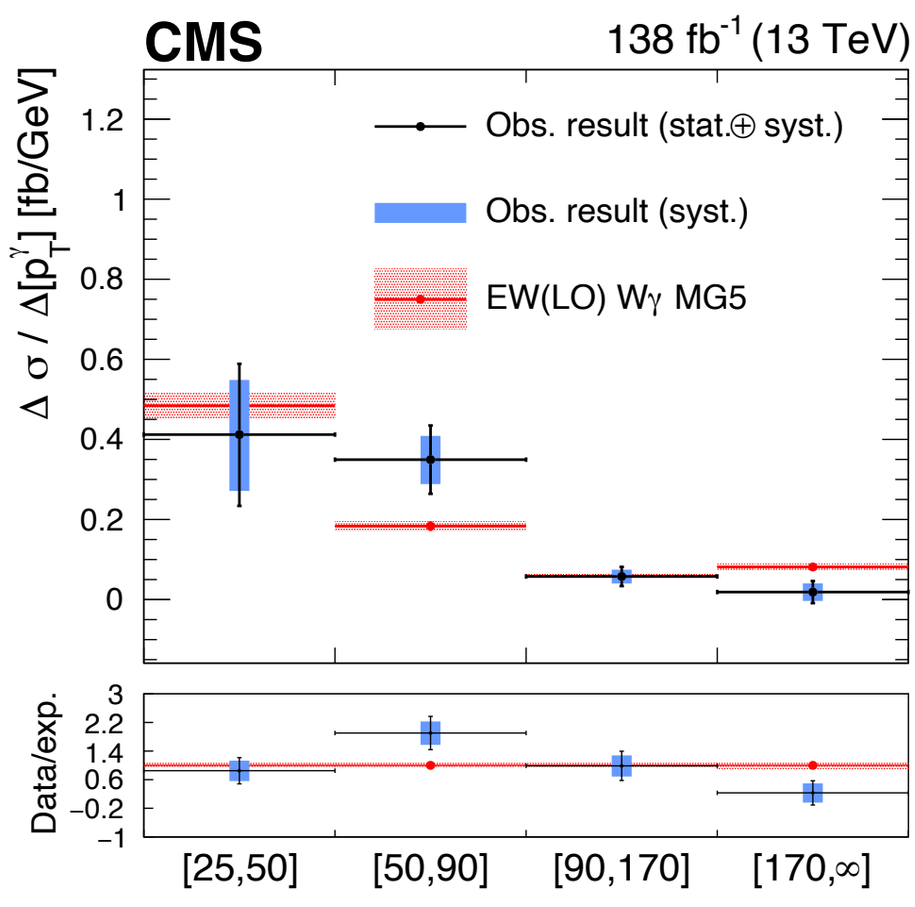

Differential cross section for the EW $W\gamma\mathrm{jj}$ production as functions of p_T^{γ}

EW $W(\ell\nu)\gamma + jj$

arXiv : 2212.12592
Accepted by PRD

- Set limit on aQGC by EFT with events in dedicated search region with high $p_T(>100\,\mathrm{GeV})$ photon.
- Fit on invariant mass of the $W\gamma$ system

All coupling parameter limits are set in TeV^{-4}, whereas the unitarity bounds are in TeV.

Expected limit	Observed limit	U_{bound}
$-5.1 < f_{M,0}/\Lambda^4 < 5.1$	$-5.6 < f_{M,0}/\Lambda^4 < 5.5$	1.7
$-7.1 < f_{M,1}/\Lambda^4 < 7.4$	$-7.8 < f_{M,1}/\Lambda^4 < 8.1$	2.1
$-1.8 < f_{M,2}/\Lambda^4 < 1.8$	$-1.9 < f_{M,2}/\Lambda^4 < 1.9$	2.0
$-2.5 < f_{M,3}/\Lambda^4 < 2.5$	$-2.7 < f_{M,3}/\Lambda^4 < 2.7$	2.7
$-3.3 < f_{M,4}/\Lambda^4 < 3.3$	$-3.7 < f_{M,4}/\Lambda^4 < 3.6$	2.3
$-3.4 < f_{M,5}/\Lambda^4 < 3.6$	$-3.9 < f_{M,5}/\Lambda^4 < 3.9$	2.7
$-13 < f_{M,7}/\Lambda^4 < 13$	$-14 < f_{M7}/\Lambda^4 < 14$	2.2
$-0.43 < f_{T,0}/\Lambda^4 < 0.51$	$-0.47 < f_{T,0}/\Lambda^4 < 0.51$	1.9
$-0.27 < f_{T,1}/\Lambda^4 < 0.31$	$-0.31 < f_{T,1}/\Lambda^4 < 0.34$	2.5
$-0.72 < f_{T,2}/\Lambda^4 < 0.92$	$-0.85 < f_{T,2}/\Lambda^4 < 1.0$	2.3
$-0.29 < f_{T,5}/\Lambda^4 < 0.31$	$-0.31 < f_{T,5}/\Lambda^4 < 0.33$	2.6
$-0.23 < f_{T,6}/\Lambda^4 < 0.25$	$-0.25 < f_{T,6}/\Lambda^4 < 0.27$	2.9
$-0.60 < f_{T,7}/\Lambda^4 < 0.68$	$-0.67 < f_{T,7}/\Lambda^4 < 0.73$	3.1

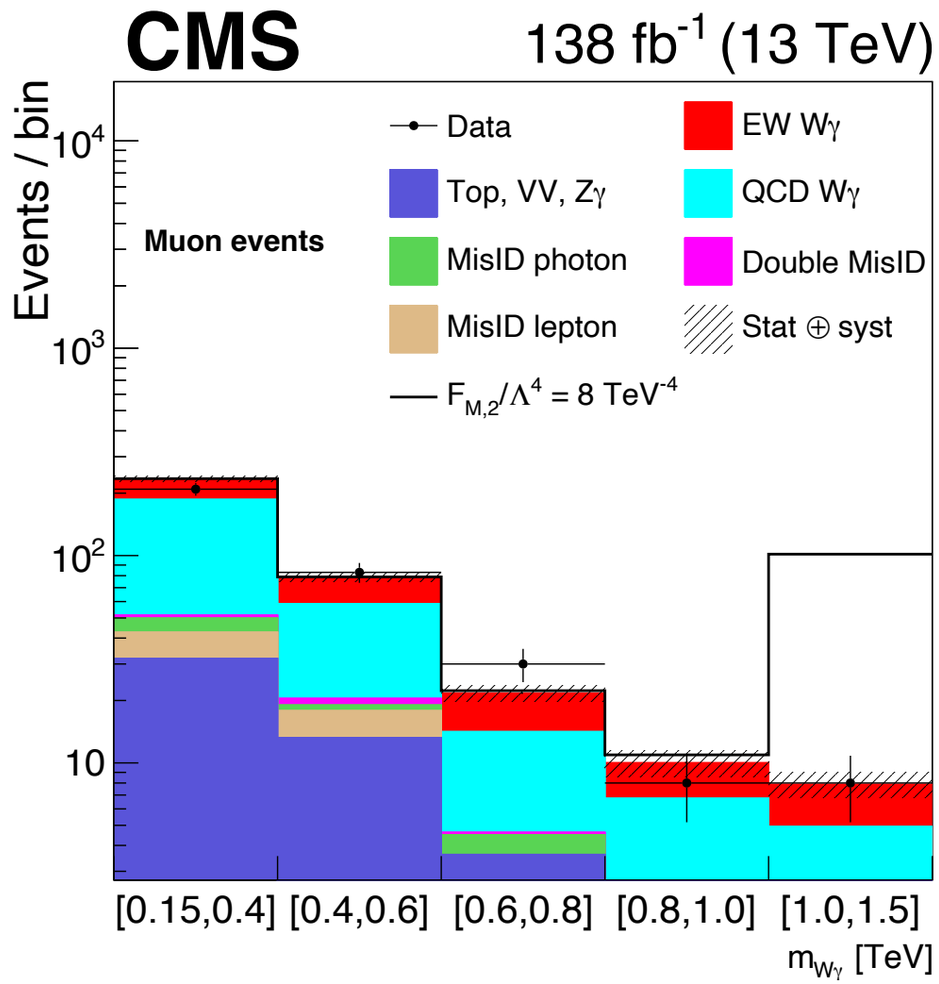

most stringent to date

	WWWW	WWZZ	ZZZZ	WWAZ	WWAA	ZZZA	ZZAA	ZAAA	AAAA
$\mathcal{O}_{S,0}$, $\mathcal{O}_{S,1}$	X	X	X						
$\mathcal{O}_{M,0}$, $\mathcal{O}_{M,1}$,$\mathcal{O}_{M,6}$,$\mathcal{O}_{M,7}$	X	X	X	X	X	X	X		
$\mathcal{O}_{M,2}$,$\mathcal{O}_{M,3}$, $\mathcal{O}_{M,4}$,$\mathcal{O}_{M,5}$		X	X	X	X	X	X		
$\mathcal{O}_{T,0}$,$\mathcal{O}_{T,1}$,$\mathcal{O}_{T,2}$	X	X	X	X	X	X	X	X	X
$\mathcal{O}_{T,5}$,$\mathcal{O}_{T,6}$,$\mathcal{O}_{T,7}$		X	X	X	X	X	X	X	X
$\mathcal{O}_{T,8}$,$\mathcal{O}_{T,9}$			X			X	X	X	X

Table 1-16. *Quartic vertices modified by each dimension-8 operator are marked with X.*

Summary

- CMS has a rich analysis program with photon object utilizing the EM calorimeter.
- The $\gamma + \text{jet}$ analysis tests QCD and feeds the PDF fits.
- The $V\gamma + \text{jj}$ analyses provides the understanding of EW sector and the possibility to search for BSM with model-independent EFT interpretation.